A&A 593, A97 (2016)
DOI: 10.1051/0004-6361/201628735

Astronomy & Astrophysics

Optical spectroscopy of Be/gamma-ray binaries

R. K. Zamanov[1], K. A. Stoyanov[1], J. Martí[2], G. Y. Latev[1], Y. M. Nikolov[1], M. F. Bode[3], and P. L. Luque-Escamilla[4]

[1] Institute of Astronomy and National Astronomical Observatory, Bulgarian Academy of Sciences, Tsarigradsko Shose 72, 1784 Sofia, Bulgaria
e-mail: rkz@astro.bas.bg
[2] Departamento de Física (EPSJ), Universidad de Jaén, Campus Las Lagunillas, A3-420, 23071 Jaén, Spain
[3] Astrophysics Research Institute, Liverpool John Moores University, IC2 Liverpool Science Park, Liverpool, L3 5RF, UK
[4] Departamento de Ingeniería Mecánica y Minera (EPSJ), Universidad de Jaén, Campus Las Lagunillas A3-008, 23071 Jaén, Spain

Received 18 April 2016 / Accepted 8 July 2016

ABSTRACT

We report optical spectroscopic observations of the Be/γ-ray binaries LSI+61303, MWC 148 and MWC 656. The peak separation and equivalent widths of prominent emission lines (Hα, Hβ, Hγ, HeI, and FeII) are measured. We estimated the circumstellar disc size, compared it with separation between the components, and discussed the disc truncation. We find that in LSI+61°303 the compact object comes into contact with the outer parts of the circumstellar disc at periastron, in MWC 148 the compact object goes deeply into the disc during the periastron passage, and in MWC 656 the black hole is accreting from the outer parts of the circumstellar disc along the entire orbit. The interstellar extinction was estimated using interstellar lines. The rotation of the mass donors appears to be similar to the rotation of the mass donors in Be/X-ray binaries. We suggest that X-ray/optical periodicity ~1 day deserves to be searched for.

Key words. stars: emission-line, Be – stars: winds, outflows – binaries: spectroscopic

1. Introduction

The rapid and sustained progress of high energy and very high energy astrophysics in recent years enabled the identification of a new group of binary stars emitting at TeV energies (e.g. Paredes et al. 2013). These objects, called γ-ray binaries, are high-mass X-ray binaries that consist of a compact object (neutron star or black hole) orbiting an optical companion that is an OB star. There are five confirmed γ-ray binaries so far: PSR B1259-63/LS 2883 (Aharonian et al. 2005), LS 5039/V479 Sct (Aharonian et al. 2006), LSI+61°303 (Albert et al. 2009), HESS J0632+057/MWC 148 (Aharonian et al. 2007), and 1FGL J1018.6-5856 (Abramowski et al. 2015). Their most distinctive fingerprint is a spectral energy distribution dominated by non-thermal photons with energies up to the TeV domain. Recently, Eger et al. (2016) proposed a binary nature for the γ-ray source HESS J1832-093/2MASS J18324516-092154 and this object probably belongs to the family of the γ-ray binaries as a sixth member.

The binary system, PSR B1259-63 is unique, since it is the only one where the compact object has been identified as a radio pulsar (Johnston et al. 1992, 1994). The nature of the compact object is known in PSR B1259-63 as a neutron star, and in AGL J2241+4454/MWC 656 as a black hole (Casares et al. 2014). Although not included in the confirmed list, MWC 656 was selected as a target here despite not having shown all the observational properties of a canonical γ-ray binary yet. It was only occasionally detected by the AGILE observatory at GeV energies and not yet detected in the TeV domain (see Aleksić et al. 2015). Nevertheless, the fact that the black hole nature of the compact companion is almost certain renders it very similar to the typical γ-ray binaries. In the other systems the nature of the compact object remains unclear (e.g. Dubus 2013). In addition to these objects, there are several other binary systems (η Car, Cyg X-1, Cyg X-3, Cen X-3, and SS 433) that are detected as GeV sources, but not as TeV sources so far.

Here we report high-resolution spectral observations of LSI+61°303, MWC 148, and MWC 656, and discuss circumstellar disc size, disc truncation, interstellar extinction, and rotation of their mass donors. The mass donors (primaries) of these three targets are emission-line Be stars. The Be stars are non-supergiant, fast-rotating B-type and luminosity class III-V stars which, at some point in their lives, have shown spectral lines in emission (Porter & Rivinius 2003). The material expelled from the equatorial belt of a rapidly rotating Be star forms an outwardly diffusing gaseous, dust-free Keplerian disc (Rivinius et al. 2013). In the optical/infrared band, the two most significant observational characteristics of Be stars and their excretion discs are the emission lines and the infrared excess. Moving along the orbit, the compact object passes close to this disc, and sometimes may even go through it causing significant perturbations in its structure. This circumstellar disc feeds the accretion disc around the compact object and/or interacts with its relativistic wind.

2. Observations

High-resolution optical spectra of the three northern Be/γ-ray binaries were secured with the fibre-fed Echelle spectrograph *ESpeRo* attached to the 2.0 m telescope of the National Astronomical Observatory Rozhen, located in Rhodope mountains, Bulgaria. The spectrograph uses R2 grating with 37.5 grooves/mm, Andor CCD camera 2048 × 2048 px, 13.5 × 13.5 μm px^{-1} (Bonev et al. 2016). The spectrograph provides a dispersion of 0.06 Å px^{-1} at 6560 Å and 0.04 Å px^{-1} at 4800 Å.

Table 1. Journal of observations.

Date-obs. yyyymmdd...hhmm	Exp-time	S/N Hα	Orb. phase
LSI+61°303			
20140217...1923	60 min	20	0.455
20140314...1746	60 min	42	0.396
20150805...0009	60 min	45	0.579
MWC 148			
20140113...1857	60 min	56	0.758
20140217...2031	60 min	44	0.870
20140218...1826	60 min	62	0.872
20140313...2002	60 min	54	0.946
20140314...1855	60 min	81	0.949
20140315...1833	60 min	46	0.952
MWC 656			
20150705...2259	30 min	55	0.691
20150804...0017	30 min	45	0.173
20150804...2229	30 min	56	0.188

The spectra were reduced in the standard way including bias removal, flat-field correction, and wavelength calibration. Pre-processing of data and parameter measurements are performed using various routines provided in IRAF. The journal of observations is presented in Table 1, where the date, start of the exposure, exposure time, and signal-to-noise ratio at about λ6600 Å are given. The orbital phases are calculated using $\mathrm{HJD}_0 = 2\,443\,366.775$, $\mathrm{HJD}_0 = 2\,454\,857.5$, and $\mathrm{HJD}_0 = 2\,453\,243.7$ for LSI+61°303, MWC 148, and MWC 656, respectively, and orbital periods given in Sect. 3.

Emission line profiles of LSI+61°303, MWC 148, and MWC 656 are plotted on Fig. 1. Spectral line parameters equivalent width (W) and distance between the peaks (ΔV) for the prominent lines (Hα, Hβ, Hγ, HeIλ5876, and FeIIλ5316) are given in Table 2. The typical error on the equivalent width is below ±10% for lines with $W > 1$ Å and up to ±20% for lines with $W \lesssim 1$ Å. The typical error on ΔV is ±10 km s^{-1}. It is worth noting that (1) in LSI+61°303 FeII lines are not detectable, (2) in MWC 656 on spectrum 20150705 the HeI λ5876 line is not visible (probably emission fills up the absorption).

In addition to the Rozhen data we use 98 spectra of MWC 148 and 68 spectra of MWC 656 (analysed in Casares et al. 2012) from the archive of the 2.0 m Liverpool Telescope[1] (Steele et al. 2004). These spectra were obtained using the Fibre-fed RObotic Dual-beam Optical Spectrograph (FRODOSpec; Morales-Rueda et al. 2004). The spectrograph is fed by a fibre bundle array consisting of 12 × 12 lenslets of 0.82 arcsec each, which is reformatted as a slit. The spectrograph was operated in a high-resolution mode, providing a dispersion of 0.8 Å px^{-1} at 6500 Å, 0.35 Å px^{-1} at 4800 Å, and typical $S/N \gtrsim 100$. FRODOSpec spectra were processed using the fully automated data reduction pipeline of Barnsley et al. (2012). The typical error on the equivalent width is ±10% and on ΔV is ±20 km s^{-1}.

[1] The Liverpool Telescope is operated on the island of La Palma by Liverpool John Moores University in the Spanish Observatorio del Roque de los Muchachos of the Instituto de Astrofisica de Canarias with financial support from the UK Science and Technology Facilities Council.

3. Objects: system parameters

LSI+61°303 (V615 Cas) was identified as a γ-ray source with the COS B satellite 35 yr ago (Swanenburg et al. 1981). For the orbital period of LSI+61°303, we adopt $P_{\rm orb} = 26.4960 \pm 0.0028$ d, which was derived with Bayesian analysis of radio observations (Gregory 2002) and an orbital eccentricity $e = 0.537$, which was obtained on the basis of the radial velocity of the primary (Casares et al. 2005; Aragona et al. 2009). For the primary, Grundstrom et al. (2007) suggested a B0V star with radius $R_1 = 6.7 \pm 0.9\ R_\odot$. A B0V star is expected to have on average $M_1 \approx 15\ M_\odot$ (Hohle et al. 2010). We adopt $v \sin i = 349 \pm 6$ km s^{-1} for the projected rotational velocity of the mass donor (Hutchings & Crampton 1981; Zamanov et al. 2013).

MWC 148 (HD 259440) was identified as the counterpart of the variable TeV source HESS J0632+057 (Aharonian et al. 2007). We adopt $P_{\rm orb} = 315^{+6}_{-4}$ d derived from the X-ray data (Aliu et al. 2014), which is consistent with the previous result of 321 ± 5 days (Bongiorno et al. 2011). For this object Aragona et al. (2010) derived $T_{\rm eff} = 27\,500$–$30\,000$ K, $\log g = 3.75$–4.00, $M_1 = 13.2$–$19.0\ M_\odot$, and $R_1 = 7.8 \pm 1.8\ R_\odot$. For the calculations in Sect. 4.2, we adopt $e = 0.83$, periastron at phase 0.967 (Casares et al. 2012), and $v \sin i = 230$–240 km s^{-1} (Moritani et al. 2015).

MWC 656 (HD 215227) is the emission-line Be star that lies within the positional error circle of the AGILE γ-ray source AGL J2241+4454 (Lucarelli et al. 2010). It is the first and until now the only detected binary composed of a Be star and a black hole (Casares et al. 2014). For the orbital period, we adopt $P_{\rm orb} = 60.37 \pm 0.04$ d obtained with optical photometry (Williams et al. 2010), $e = 0.10 \pm 0.04$ estimated on the basis of the radial velocity measurements and $v \sin i = 330 \pm 30$ km s^{-1} (Casares et al. 2014). For the primary, Williams et al. (2010) estimated $T_{\rm eff} = 19\,000 \pm 3000$ K, $\log g = 3.7 \pm 0.2$, $M_1 = 7.7 \pm 2.0\ M_\odot$, $R_1 = 6.6 \pm 1.9\ R_\odot$. Casares et al. (2014) considered that the mass donor is a giant (B1.5-2 III) and give a mass range $M_1 = 10$–$16\ M_\odot$. On average a B1.5-2 III star is expected to have about $R_1 \approx 8.3$–$8.8\ R_\odot$ (Straizys & Kuriliene 1981). From newer values of the luminosity (Hohle et al. 2010), such a star is expected to have $M_1 \approx 8.0$–$10.0\ M_\odot$ and radius $R_1 \approx 9.5$–$10\ R_\odot$. We adopt $R_1 \approx 10\ R_\odot$ for the calculations in Sect. 4.2.

4. Circumstellar disc

4.1. Peak separation in different lines

For the Be stars, the peak separations in different lines follow approximately the relations (Hanuschik et al. 1988)

$$\Delta V_\beta \approx 1.8 \Delta V_\alpha \quad (1)$$

$$\Delta V_\gamma \approx 1.2 \Delta V_\beta \approx 2.2 \Delta V_\alpha \quad (2)$$

$$\Delta V_{\rm FeII} \approx 2.0 \Delta V_\alpha \quad (3)$$

$$\Delta V_{\rm FeII} \approx 1.1 \Delta V_\beta, \quad (4)$$

where Eq. (4) is derived from Eqs. (1) and (3).

For LSI+61°303 using the measurements in Table 2, we obtain $\Delta V_\beta = 1.30 \pm 0.04\,\Delta V_\alpha$ and $\Delta V_{\rm HeI5876} = 1.38 \pm 0.13\,\Delta V_\alpha$. The ratio $\Delta V_\beta / \Delta V_\alpha$ is considerably below the average value for the Be stars (see Eq. (1)).

We obtain $\Delta V_\beta = 1.78 \pm 0.06\,\Delta V_\alpha$, $\Delta V_\gamma = 1.07 \pm 0.03\,\Delta V_\beta$, and $\Delta V_{\rm FeII5316} = 1.12 \pm 0.03\,\Delta V_\beta$, $\Delta V_{\rm HeI5876} = 1.47 \pm 0.10\,\Delta V_\beta$ for MWC 148. We use only three spectra for Hα (20 140 113, 20 140 217, and 20 140 218) when two peaks in Hα are visible.

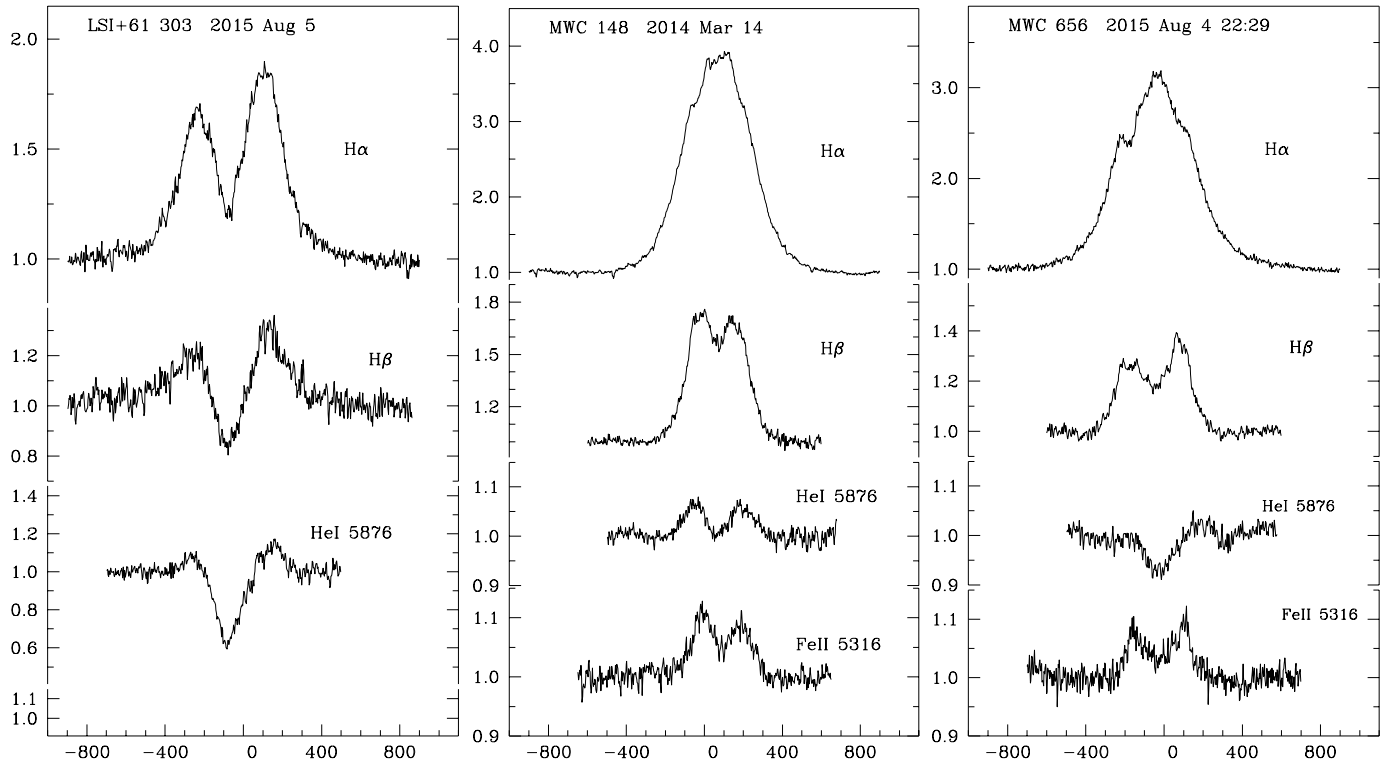

Fig. 1. Emission line profiles of LSI+61°303, MWC 148, and MWC 656.

Table 2. Spectral line parameters.

Object	Hα		Hβ		Hγ		HeI 5876		FeII 5316	
date-obs	W_α	ΔV_α	W_β	ΔV_β	W_γ	ΔV_γ	$W_{\rm HeI5876}$	$\Delta V_{\rm HeI5876}$	$W_{\rm FeII5316}$	$\Delta V_{\rm FeII}$
yyyymmdd.hhmm	Å	km s^{-1}	Å	km s^{-1}	Å	km s^{-1}	Å	km s^{-1}	Å	km s^{-1}
LSI+61°303										
20140217.1923	–8.6	316	–0.71	416	+0.5	...	+0.39	455	...	...
20140314.1746	–8.1	309	–1.12	411	+0.7	...	+0.17	456	...	...
20150805.0009	–8.2	337	–1.16	421	+0.8	...	+0.40	416	...	...
MWC 148										
20140113.1857	–29.5	105	–4.19	182	–1.38	188	–0.49	231	–0.49	210
20140217.2031	–30.9	92	–4.27	162	–1.24	178	–0.37	243	–0.37	177
20140218.1826	–29.3	87	–4.12	161	–1.12	171	–0.39	244	–0.39	182
20140313.2002	–29.0	...	–3.41	165	–0.77	149	–0.39	246	–0.39	186
20140314.1855	–28.5	...	–3.79	170	–1.04	159	–0.37	251	–0.37	185
20140315.1833	–26.8	...	–3.84	168	–1.01	175	–0.51	264	–0.51	186
MWC 656										
20150705.2259	–23.3	...	–2.26	246	–0.42	301	+0.0	...	–0.40	275
20150804.0017	–21.9	...	–2.12	244	–0.23	289	+0.22	...	–0.48	240
20150804.2229	–21.2	...	–1.98	246	–0.34	311	+0.19	...	–0.42	227

The value of $\Delta V_\beta/\Delta V_\alpha \approx 1.78$ is very similar to 1.8 in Be stars, the ratio $\Delta V_{\rm FeII5316}/\Delta V_\beta \approx 1.07$ is similar to 1.1 in Be stars, and the value of $\Delta V_\gamma/\Delta V_\beta \approx 1.07$ is again similar to the value 1.2 for Be stars.

We estimate $\Delta V_\beta = 1.72 \pm 0.18\, \Delta V_\alpha$ for MWC 656 (using six spectra from the Liverpool Telescope FRODOSpec, where two peaks are visible in both Hα and Hβ), $\Delta V_\gamma = 1.22 \pm 0.04\, \Delta V_\beta$, $\Delta V_{\rm FeII5316} = 1.01 \pm 0.10\, \Delta V_\beta$, where all three ratios are similar to the corresponding values (Eq. (1), (2), (4)) in Be stars. We do not see two peaks on high-resolution Rozhen spectra of this object. However two peaks are clearly distinguishable on a few of the LT spectra. In every case of detection/non-detection of the double peak structure, Wα is very similar $19 <$ W$\alpha <$ 25 Å.

The comparison of the peak separation of different emission lines shows that MWC 148 and MWC 656 have circumstellar disc that is similar to that of the normal Be stars. At this stage considerable deviation from the behaviour of the Be stars is only detected in LSI+61°303. In this star the Hα-emitting disc is only 1.7 times larger than the Hβ-emitting disc, while in normal Be stars it is 3.3 times larger. This probably is one more

Table 3. Disc size in different emission lines.

Date-obs. yyyymmdd.hhmm	$R_{\rm disc}$(Hα) $R_\odot$ (^{a})	$R_{\rm disc}$(Hα) $R_\odot$ (^{b})	$R_{\rm disc}$(Hα) $R_\odot$ (^{c})	$R_{\rm disc}$(Hβ) $R_\odot$	$R_{\rm disc}$(Hγ) $R_\odot$	$R_{\rm disc}$(HeI5876) $R_\odot$	$R_{\rm disc}$(FeII) $R_\odot$
LSI+61°303							
20140217.1923	33	32	36	19	...	16	...
20140314.1746	34	33	33	19	...	16	...
20150805.0009	29	31	34	18	...	19	...
MWC 148							
20140113.1857	156	165	180	52	49	32	39
20140217.2031	205	208	190	66	54	29	55
20140218.1826	226	211	178	66	59	29	52
20140313.2002	...	201	176	63	52	29	50
20140314.1855	...	189	172	60	56	27	50
20140315.1833	...	193	160	60	50	25	50
MWC 656							
20150705.2259	...	213	174	63	42	...	51
20150804.0017	...	216	162	64	46	...	66
20150804.2229	...	213	156	63	40	...	74

Notes. (^{a}) Calculated using ΔV_α and Eq. (5). (^{b}) Calculated using ΔV_β and Eq. (5). (^{c}) Calculated using W_α and Eq. (8).

indication that outer parts of the disc are truncated as a result of the relatively short orbital period.

4.2. Disc size

For rotationally dominated profiles, the peak separation can be regarded as a measure of the outer radius ($R_{\rm disc}$) of the emitting disc (Huang 1972)

$$\left(\frac{\Delta V}{2\,v\,\sin i}\right) = \left(\frac{R_{\rm disc}}{R_1}\right)^{-j}, \quad (5)$$

where $j = 0.5$ for Keplerian rotation, $j = 1$ for angular momentum conservation, R_1 is the radius of the primary, and $v\,\sin i$ is its projected rotational velocity. Equation (5) relies on the assumptions that (1) the Be star is rotating critically, and (2) that the line profile shape is dominated by kinematics and radiative transfer does not play a role.

When the two peaks are visible in the emission lines, we can estimate the disc radius using Eq. (5). The calculated disc size for different emission lines are given in Table 3.

In the Hα emission line of LSI+61°303 two peaks are clearly visible on all of our spectra. However in MWC 656 the Hα emission line seems to exhibit three peaks (see Fig. 1). Two peaks in Hα emission of MWC 148 are clearly detectable on January-February 2014 observations. Two peaks are not distinguishable on the spectra obtained in March 2014 (when the companion is at periastron), which probably indicates perturbations in the outer parts of the disc caused by the orbital motion of the compact object.

In the Hβ line two peaks are visible on all the Rozhen spectra. We take this opportunity to obtain an estimation of the $R_{\rm disc}$(Hα) using ΔV_β; the ratios $\Delta V_\beta/\Delta V_\alpha$ (as obtained in Sect. 4.1), and Eq. (5). The $R_{\rm disc}$(Hα) values calculated in this way are given in Table 3 and indicated with (^{b}).

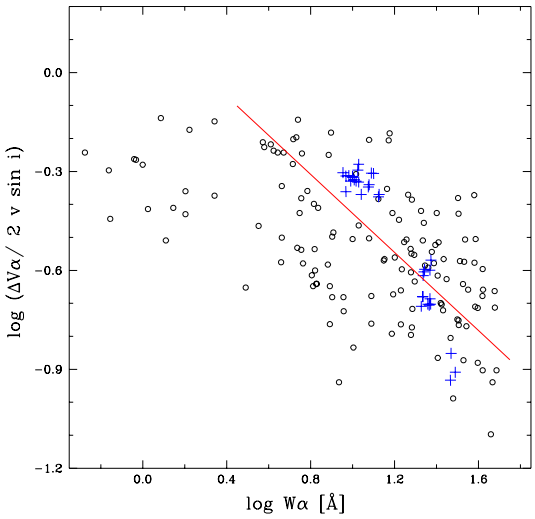

Fig. 2. Distance between the peaks of Hα emission line (normalized with stellar rotation and inclination) versus W_α on a logarithmic scale. Black empty circles indicate normal Be stars, red pluses indicate Be/γ-ray binaries. The solid line denotes $y = -0.592\,x + 0.165$ (see Sect. 4.3).

4.3. Disc size and W_α

The disc size and W_α are connected (see also Hanuschik 1989; Grundstrom & Gies 2006). This simply expresses the fact that $R_{\rm disc}$ grows as W_α becomes larger. In Fig. 2, we plot $\log \Delta V_\alpha/2v\,\sin\,i$ versus $\log W_\alpha$. In this figure 138 data points are plotted for Be stars taken from Andrillat (1983), Hanuschik (1986), Hanuschik et al. (1988), Dachs et al. (1992), Slettebak et al. (1992), and Catanzaro (2013). In this figure, the data for Be/γ-ray binaries are also plotted. The three Be/γ-ray binaries are inside the distribution of normal Be stars.

There is a moderate to strong correlation between the variables with Pearson correlation coefficient −0.63, Spearman's (rho) rank correlation 0.64, and p-value $\sim 10^{-15}$. The

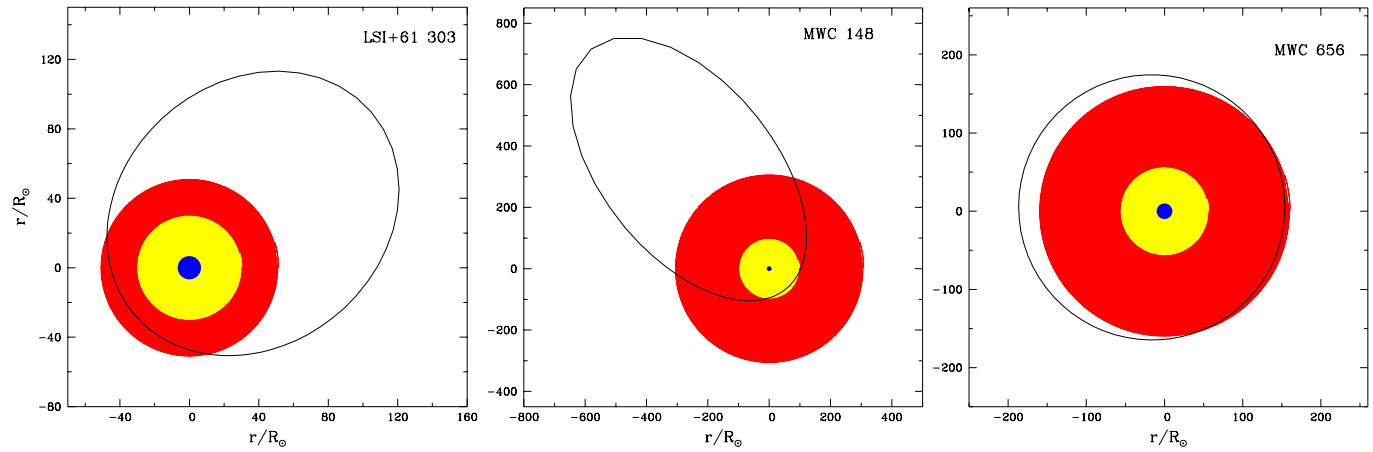

Fig. 3. Orbit of the compact object and circumstellar disc for LSI+61°303, MWC 148, and MWC 656. Red indicates the disc size in Hα, yellow indicates the disc size in Hβ. The blue circle indicates the size of the mass donor. We have three different cases: the orbit crossing the outer parts of the disc (LSI+61°303), the orbit entering deeply in the disc at periastron (MWC 148), and the orbit at the disc border (MWC 656).

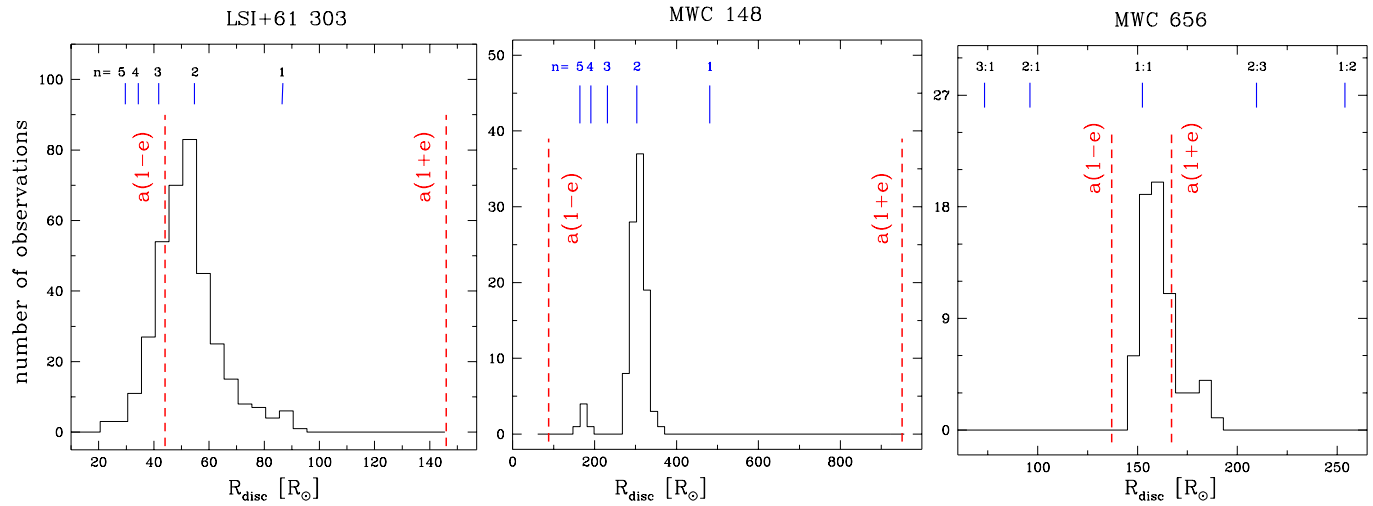

Fig. 4. Histograms of the disc size. The vertical dashed (red) lines indicate the distance between the components at periastron and apastron, $a(1-e)$ and $a(1+e)$, respectively. The resonances n:m are also indicated (in blue). For LSI+61°303 and MWC 148 only those with $m = 1$ are given.

dependence is of the form

$$\log\left(\Delta V_\alpha / 2v \sin i\right) = -a \ \log W_\alpha + b, \tag{6}$$

and the slope is shallower for stars with $W_\alpha < 3$ Å as noted by Hanuschik et al. (1988). For 120 data points in the interval $3 \leq W_\alpha \leq 50$ Å, using a least-squares approximation we calculate $a = 0.592 \pm 0.030$ and $b = 0.165 \pm 0.036$. This fit as well as the correlation coefficients are calculated using only normal Be stars. Using Eqs. (5) and (6) we then obtain

$$\left(\frac{R_{\rm disc}}{R_1}\right)^{-j} = 1.462 \ W_\alpha^{-0.592}. \tag{7}$$

Having in mind that (1) the discs of the Be stars are near Keplerian (Porter & Rivinius 2003, Meilland et al. 2012); (2) the Be stars rotate at rates below the critical rate (e.g. Chauville et al. 2001), and (3) at higher optical depths the emission line peaks are shifted towards lower velocities (Hummel & Dachs 1992), we calculate the disc radius with the following formula:

$$\frac{R_{\rm disc}}{R_1} = \epsilon \ 0.467 \ \ W_\alpha^{1.184}, \tag{8}$$

where ϵ is a dimensionless parameter (see also Zamanov et al. 2013), for which we adopt $\epsilon = 0.9 \pm 0.1$. The disc sizes calculated with Eq. (8) are given in Table 3 and are denoted with (^{c}). As can be seen, the values agree with those obtained with the conventional method. We estimate average values of the dimensionless quantity $R_{\rm disc}/\epsilon R_1 = 8.7 \pm 1.9$ (for LSI+61°303), $R_{\rm disc}/\epsilon R_1 = 43 \pm 5$ (for MWC 148), and $R_{\rm disc}/\epsilon R_1 = 18.0 \pm 1.1$ (for MWC 656), respectively.

4.4. Disc truncation

The orbit of the compact object, the average size of Hα disc, the average size of Hβ disc, and the Be star are plotted in Fig. 3. The coordinates X and Y are in solar radii. The histograms of Hα disc size, calculated using Eq. (8), are plotted in Fig. 4. For LSI+61°303, we use our new data and published data from Paredes et al. (1994), Steele et al. (1996), Liu & Yan (2005), Grundstrom et al. (2007), McSwain et al. (2010), and Zamanov et al. (1999, 2013). We use Rozhen and Liverpool Telescope spectra for MWC 148 and MWC 656. In all three stars the distribution of $R_{\rm disc}$ values has a very well pronounced peak. The tendency for the disc emission fluxes to cluster at specified levels is related to the truncation of the disc at specific disc radii

by the orbiting compact object (e.g. Coe et al. 2006). Okazaki & Negueruela (2001) proposed that these limiting radii are defined by the closest approach of the companion in the high-eccentricity systems and by resonances between the orbital period and the disc gas rotational periods in the low-eccentricity systems. The resonance radii are given by

$$R_{n:m}^{3/2} = \frac{m\,(G\,M_1)^{1/2}}{2\,\pi}\,\frac{P_{\rm orb}}{n}, \quad (9)$$

where G is the gravitational constant, n is the integer number of disc gas rotational periods, and m is the integer number of orbital periods. The important resonances are not only those with n:1, but can also be n:m in general.

For LSI+61°303 (assuming $M_1 \approx 15\ M_\odot$, $M_2 \approx 1.4\ M_\odot$, $e \approx 0.537$), we estimate the distances between the components $a(1-e) \approx 44\ R_\odot$ and $a(1+e) \approx 146\ R_\odot$ for the periastron and apastron, respectively. As can be seen from Fig. 4, the disc size is $R_{\rm disc} \sim a(1-e)$ and it never goes close to $a(1+e)$. The resonances that correspond to disc size are between 5:1 and 1:1, and the peak on the histogram corresponds to the 2:1 resonance.

For MWC 148, with the currently available data ($M_1 \approx 15\ M_\odot$, $M_2 \approx 4\ M_\odot$, $e \approx 0.83$), we estimate $a(1-e) \approx 88\ R_\odot$ and $a(1+e) \approx 951\ R_\odot$ for the periastron and apastron, respectively. In Fig. 4, it is apparent that $a(1-e) < R_{\rm disc} < a(1+e)$. The 2:1 resonance is the closest to the peak of the distribution. We note in passing that the disc size in this star could have a bimodal distribution (a second peak with lower intensity seems to emerge close to 4:1 resonance radius).

For MWC 656 (assuming $M_1 \approx 9\ M_\odot$, $M_2 \approx 4\ M_\odot$, $e \approx 0.1$), we estimate $a(1-e) \approx 137\ R_\odot$ and $a(1+e) \approx 167\ R_\odot$ for the periastron and apastron, respectively. In Fig. 4, it is seen that the 1:1 resonance is very close to the peak of the distribution and $a(1-e) \lesssim R_{\rm disc} \lesssim a(1+e)$. The disc size rarely goes above $a(1+e)$.

5. Interstellar extinction: estimates of *E(B – V)* from interstellar lines

There is a strong correlation between equivalent width of the diffuse interstellar bands (DIBs) and reddening (Herbig 1975; Puspitarini et al. 2013). There is also a calibrated relation of reddening with the equivalent width of the interstellar line $KI\lambda7699$ Å (Munari & Zwitter 1997). Aiming to estimate the interstellar extinction towards our objects, we measure equivalent widths of $KI\lambda7699$ Å and DIBs $\lambda6613$, $\lambda5780$, $\lambda5797$.

LSI+61°303: for this object, Hunt et al. (1994) use $E(B-V) = 0.93$ (Hutchings & Crampton 1981). Howarth (1983) using the 2200 Å extinction bump obtained $E(B-V) = 0.75 \pm 0.1$. Steele et al. (1998) estimated $E(B-V) = 0.70 \pm 0.40$ from Na I D_2 and $E(B-V) = 0.65 \pm 0.25$ from diffuse interstellar bands. For LSI+61°303, we measure $0.17 \leq W(KI\lambda7699) \leq 0.19$ Å, $0.17 < W(DIB\lambda6613) < 0.19$ Å, $0.34 < W(DIB\lambda5780) < 0.41$ Å, $0.09 < W(DIB\lambda5797) < 0.16$ Å, which following Munari & Zwitter (1997) and Puspitarini et al. (2013) calibrations corresponds to $E(B-V) = 0.84 \pm 0.08$.

MWC 148: for this star, Friedemann (1992) estimated $E(B-V) = 0.85$ from the 217 nm band. We measure $0.14 < W(KI\lambda7699) < 0.20$ Å, $0.13 < W(DIB\lambda6613) < 0.18$ Å, $0.28 < W(DIB\lambda5780) < 0.34$ Å, $0.13 < W(DIB\lambda5797) < 0.15$ Å, which corresponds to a slightly lower value $E(B-V) = 0.77 \pm 0.06$.

MWC 656: for this star, Williams et al. (2010) gave a low value $E(B-V) = 0.02$. Casares et al. (2014) estimated $E(B-V) = 0.24$. We measure $0.04 < W(DIB\lambda6613) < 0.06$ Å, $0.09 \leq W(DIB\lambda5780) \leq 0.10$ Å, $0.03 < W(DIB\lambda5797) < 0.05$ Å, and estimate $E(B-V) = 0.25 \pm 0.02$.

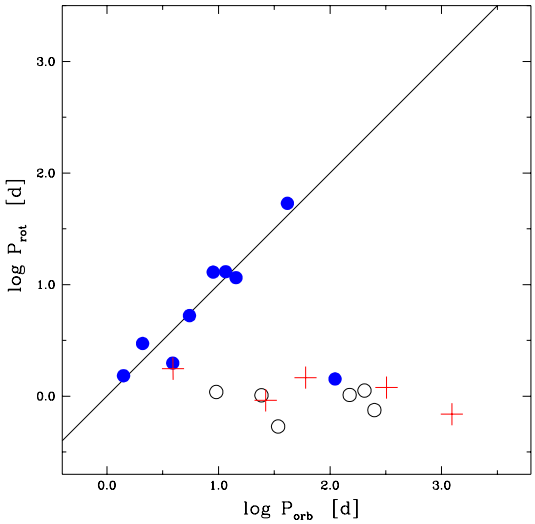

Fig. 5. Rotational period of the mass donor ($P_{\rm rot}$) vs. $P_{\rm orb}$. Filled (blue) circles indicate high-mass X-ray binaries with giant/supergiant mass donor, open circles indicate Be/X-ray binaries, and red plusses indicate γ-ray binaries.

6. Rotational period of the mass donors

In close binary systems the rotation of the companions of compact objects is accelerated by mass transfer and tidal forces (e.g. Ablimit & Lü 2012). Adopting the parameters given in Sect. 3, we estimate the rotational periods of the mass donors $P_{\rm rot} \approx 0.92$ d (for LSI+61°303), $P_{\rm rot} \approx 0.91$ d (MWC 148), and $P_{\rm rot} \approx 0.86$ d (MWC 656).

For the γ-ray binary LS 5039, the mass donor is a O6.5V((f)) star with $R_1 = 9.3 \pm 0.6\ R_\odot$, inclination $i \approx 24.9°$, $v \sin i = 113 \pm 8$ km s^{-1} (Casares et al. 2005). We calculate $P_{\rm rot} = 1.764$ d. Because of the short orbital period $P_{\rm orb} = 3.91$ d, the rotation of the mass donor could be pseudo-synchronized with the orbital motion (Casares et al. 2005).

Radio observations of the pulsar in PSR B1259-63/LS 2883 allow the orbital parameters to be precisely established: $P_{\rm orb} = 1236.72$ d and eccentricity of $e = 0.87$ (Wang et al. 2004; Shannon et al. 2014). For the primary, Negueruela et al. (2011) estimated $R_1 = 9.0 \pm 1.5\ R_\odot$, $v \sin i = 260 \pm 15$ km s^{-1}, and $i_{\rm orb} \approx 23°$, which give $P_{\rm rot} = 0.689$ d.

In Fig. 5 we plot $P_{\rm rot}$ versus $P_{\rm orb}$ for a number of high-mass X-ray binaries (see also Stoyanov & Zamanov 2009). High-mass X-ray binaries with a giant/supergiant component, Be/X-ray binaries, and Be/γ-ray binaries are plotted with different symbols in this figure. The solid line represents synchronization ($P_{\rm rot} = P_{\rm orb}$). Among the five γ-ray binaries with known rotational velocity of the mass donor, the rotation of the mass donor is close to synchronization with the orbital motion in only one (LS 5039). The four Be/γ-ray binaries are not close to the line of synchronization. They occupy the same region as the Be/X-ray binaries; in other words regarding the rotation of the mass donor the Be/γ-ray binaries are similar to the Be/X-ray binaries. In these, the tidal force of the compact object acts to decelerate the rotation of the mass donor. The spin-down of the Be stars due to angular momentum transport from star to disc (Porter 1998) is another source of deceleration.

In the well-known Be star γ Cas, Robinson & Smith (2000) found that the X-ray flux varied with a period $P = 1.1$ d, which they interpreted as the rotational period of the mass donor. A similar period is detected in photometric observations (Harmanec et al. 2000; Henry & Smith 2012). This periodicity is probably due to the interaction between magnetic field of the Be star and its circumstellar disc or the presence of some physical feature, such as a spot or cloud, co-rotating with the star. The optical emission lines of MWC 148 are practically identical to those of γ Cas. All detected lines in the observed spectral range (Balmer lines, HeI lines and FeII lines) have similar equivalent widths, intensities, profiles, and even a so-called wine-bottle structure noticeable in the Hα line (see Fig. 1 in Zamanov et al. 2016). Bearing in mind the above estimations and the curious similarities between: (i) the mean 20−60 keV X-ray luminosity of γ Cas and LSI+61°303 (Shrader et al. 2015) and (ii) the optical emission lines of γ Cas and MWC 148, we consider that periodicity ∼1 day could be detectable in X-ray/optical bands in the Be/γ-ray binaries and could provide a direct measurement of the rotational period of the mass donor.

7. Discussion

The three Be/γ-ray binaries discussed here have non-zero eccentricities and misalignment between the spin axis of the star and the spin axis of the binary orbit could be possible (Martin et al. 2009).

The inclination of the primary star in LSI+61°303 to the line of sight is probably $iB_{\rm Be} \sim 70°$ (Zamanov et al. 2013). Aragona et al. (2014) derived $a_1 \sin i_{\rm orb} = 8.64 \pm 0.52$. Assuming $M_1 = 15\ M_\odot$, $M_2 = 1.4\ M_\odot$, we estimate $i_{\rm orb} \sim 67°-73°$. It appears that there is no significant deviation of the orbital plane from the equatorial plane of the Be star.

The emission lines of MWC 148 are very similar to those of γ Cas. The emission lines are most sensitive to the footpoint density and inclination angle (Hummel 1994). It means that in MWC 148 the Be star inclination should be similar to that of γ Cas, for which the inclination is in the range 40°−50° (Clarke 1990, Quirrenbach et al. 1997). For MWC 148, Casares et al. (2012) estimated $a_1 \sin i_{\rm orb} = 77.6 \pm 25.9$, which for $M_1 = 15\ M_\odot$ and a 4 $M_\odot$ black hole gives $45° \lesssim i_{\rm orb} \lesssim 65°$.

For MWC 656, Casares et al. (2014) give $M_1 \sin^3 i_{\rm orb} = 5.83 \pm 0.70$. Bearing in mind the range of $8\ M_\odot \leq M_1 \leq 10\ M_\odot$, this gives $53° \lesssim i_{\rm orb} \lesssim 59°$. Inclination of the Be star can be evaluated from the full width at zero intensity of the FeII lines $FWZI/2 \sin i = (GM_1/R_1)^{1/2}$. From FWZI of FeII lines (Casares et al. 2012) and using $R_1 = 9.5-10.0\ R_\odot$ we estimate $iB_{\rm Be} \approx 53-61°$. It appears that both planes are almost complanar.

There are no signs of considerable deviation between the two planes. The opening half-angle of the Be stars' circumstellar disc are ∼10° (Tycner et al. 2006; Cyr et al. 2015) and it means that the compact object is practically orbiting in the plane of the circumstellar disc. The comparison between the orbit and circumstellar disc size (see Fig. 3 and Sect. 4.4) shows that in these three objects we have three different situations:

- In LSI+61°303 the neutron star passes through the outer parts of the circumstellar disc at periastron, but it does not enter deeply in the disc;
- In MWC 148 the compact object goes into the innermost parts of the disc (passes through the innermost parts and penetrates deeply in the disc) during the periastron passage;
- In MWC 656 the black hole is constantly accreting from the outer edge of the circumstellar disc.

In MWC 656, this means that the compact object (black hole) is at the disc border at all times and as a consequence it will have a higher and stable mass accretion rate along the entire orbit. It seems to be a very clear case of disc truncation in which the circumstellar disc is cut almost exactly at the black hole orbit.

Because the Hα peaks are connected with the outermost parts of the disc, the above three items probably explain the observational findings:

1. In LSI+61°303 the Hα emission line has a two-peak profile at all times (in all our spectra in the period 1987−2015),because the circumstellar disc size is relatively small and the neutron star passes only through the outermost parts of the circumstellar disc at periastron;
2. In MWC 148, the big jumps in the Hα parameters, W_α, full width at half maximum and radial velocity (see Fig. 4 of Casares 2012) occur because the compact object enters (reaches) the inner parts of the disc during the periastron passage.
3. In MWC 656 the double-peak profile is not often visible because the black hole is at the outer edge at all times and makes perturbations exactly in the places where the Hα peaks are formed.

It is worth noting that when the compact object causes large-scale perturbations, distorted profiles, such as those observed in 1A 535+262 (Moritani et al. 2011, 2013), will appear. If only a small portion of the outer disc is perturbed then it will appear in the central part of the emission line profile (e.g. in between the peaks or even filling the central dip) because the outer parts of the disc produce the central part of the Hα emission line profile. Similar additional emission is already detected in the Hα spectra of LSI+61°303 (Paredes et al. 1990; Liu et al. 2000; Zamanov & Marti 2000).

Gamma-ray emission has been repeatedly observed to be periodic in the system LSI+61303 (Albert et al. 2009; Saha et al. 2016) and also very likely in MWC148, where its periodic X-ray flares are highly correlated with TeV emission (Aliu et al. 2014). A similar situation occurs in the case of LS 5039 (Aharonian et al. 2006), 1FGL J1018.6-20135856 (Abramowski et al. 2015), and PSR B1259-63 (Abramowski et al. 2013), which has the longest orbital period observed in a γ-ray binary (about 3 yr). This is likely related to the very different physical conditions sampled by the compact companion as it revolves around the primary star in an eccentric orbit. Non-thermal emission (e.g. Dubus 2013) is produced from particles accelerated at the shock between the wind of the pulsar and matter flowing out from the primary star (the polar wind as well as the disc).

The X-ray and γ-ray light curve of MWC 148 shows two maxima at orbital phases 0.35 and 0.75 and minimum at apastron passage (Acciari et al. 2009; Aliu et al. 2014). X-ray and γ-ray fluxes are correlated as mentioned above, in agreement with leptonic emission models, where relativistic electrons lose energy by synchrotron emission and inverse Compton emission (Maier & the VERITAS Collaboration 2015). The highly eccentric orbital geometry sketched in the central panel of Fig. 3 is also in good agreement with a periodic flaring system.

In the case of MWC 656, γ-rays have been detected occasionally (Williams et al. 2010), but so far never reaching the TeV energy domain. The main differences from previous sources are the fact that the compact object has been shown to be a black hole and its orbit is only moderately eccentric (Casares et al. 2014). Based on our spectroscopic observations, the size of the excretion disc is such that the black hole is accreting matter only from its lower density outer edges. As mentioned before,

this implies that the accretion rate is stable but at the same time low. Indeed, the quiescent X-ray emission level of the system is as weak as $\sim 10^{-8}$ Eddington luminosity (Munar-Adrover et al. 2014). Therefore, episodic γ-ray flares such as those detected by AGILE, likely require some enhancement of mass loss from the primary Be star or clumps in its circumstellar disc. We speculate here that the physical mechanism responsible for γ-ray emission in the MWC 656 black hole context could be related to the alternative microquasar-jet scenario also proposed for γ-ray binaries (see e.g. Romero et al. 2007). The fact that MWC 656 seems to adhere to the low-luminosity end of the X-ray/radio correlation for hard state compact jets also points in this direction (Dzib et al. 2015).

8. Conclusions

From the spectroscopic observations of the three Be/γ-ray binaries we deduce that in LSI+61°303 the neutron star crosses the outer parts of the circumstellar disc at periastron, in MWC 148 the compact object passes deeply through the disc during the periastron passage, and in MWC 656 the black hole is accreting from the outer parts of the circumstellar disc during the entire orbital cycle. The histograms in all three stars show that the disc size clusters at specific levels, indicating the circumstellar disc is truncated by the orbiting compact object. We estimate the interstellar extinction towards LSI+61°303, MWC 148, and MWC 656. The rotation of the mass donors is similar to that of the Be/X-ray binaries. We suggest that the three stars deserve to be searched for a periodicity of about 1.0 day.

Acknowledgements. The authors are grateful to an anonymous referee for valuable comments and suggestions. This work was partially supported by grant AYA2013-47447-C3-3-P from the Spanish Ministerio de Economía y Competitividad (MINECO), and by the Consejería de Economía, Innovación, Ciencia y Empleo of Junta de Andalucía as research group FQM-322, as well as FEDER funds.

References

Ablimit, I., & Lü, G. L. 2012, Sci. China Phys. Mech. Astron. 56, 663
Abramowski, A., Acero, F., et al. (H.E.S.S. Collaboration) 2013, A&A, 551, A94
Abramowski, A., Aharonian, F., et al. (H.E.S.S. Collaboration) 2015, A&A, 577, A131
Acciari, V. A., Aliu, E., Arlen, T., et al. 2009, ApJ, 698, L94
Aharonian, F., Akhperjanian, A. G., Aye, K.-M., et al. 2005, A&A, 442, 1
Aharonian, F., Akhperjanian, A. G., Bazer-Bachi, A. R., et al. 2006, A&A, 460, 743
Aharonian, F. A., Akhperjanian, A. G., Bazer-Bachi, A. R., et al. 2007, A&A, 469, L1
Albert, J., Aliu, E., Anderhub, H., et al. 2009, ApJ, 693, 303
Aleksić, J., Ansoldi, S., Antonelli, L. A., et al. 2015, A&A, 576, A36
Aliu, E., Archambault, S., Aune, T., et al. 2014, ApJ, 780, 168
Andrillat, Y. 1983, A&AS, 53, 319
Aragona, C., McSwain, M. V., Grundstrom, E. D., et al. 2009, ApJ, 698, 514
Aragona, C., McSwain, M. V., & De Becker, M. 2010, ApJ, 724, 306
Barnsley, R. M., Smith, R. J., & Steele, I. A. 2012, Astron. Nachr., 333, 101
Bongiorno, S. D., Falcone, A. D., Stroh, M., et al. 2011, ApJ, 737, L11
Bonev, T., Markov, H., Bogdanovski, R., et al. 2016, Bulg. Astron. J., in press
Casares, J., Ribó, M., Ribas, I., et al. 2005, MNRAS, 364, 899
Casares, J., Ribó, M., Ribas, I., et al. 2012, MNRAS, 421, 1103
Casares, J., Negueruela, I., Ribó, M., et al. 2014, Nature, 505, 378
Catanzaro, G. 2013, A&A, 550, A79
Chauville, J., Zorec, J., Ballereau, D., et al. 2001, A&A, 378, 861
Clarke, D. 1990, A&A, 227, 151
Coe, M. J., Reig, P., McBride, V. A., Galache, J. L., & Fabregat, J. 2006, MNRAS, 368, 447
Cyr, R. P., Jones, C. E., & Tycner, C. 2015, ApJ, 799, 33
Dachs, J., Hummel, W., & Hanuschik, R. W. 1992, A&AS, 95, 437
Dubus, G. 2013, A&ARv, 21, 64
Dzib, S. A., Massi, M., & Jaron, F. 2015, A&A, 580, L6
Eger, P., Laffon, H., Bordas, P., et al. 2016, MNRAS, 457, 1753
Friedemann, C. 1992, Bulletin d'Information du Centre de Données Stellaires, 40, 31
Gregory, P. C. 2002, ApJ, 575, 427
Grundstrom, E. D., & Gies, D. R. 2006, ApJ, 651, L53
Grundstrom, E. D., Caballero-Nieves, S. M., Gies, D. R., et al. 2007, ApJ, 656, 437
Harmanec, P., Habuda, P., Štefl, S., et al. 2000, A&A, 364, L85
Hanuschik, R. W. 1986, A&A, 166, 185
Hanuschik, R. W. 1989, Ap&SS, 161, 61
Hanuschik, R. W., Kozok, J. R., & Kaiser, D. 1988, A&A, 189, 147
Henry, G. W., & Smith, M. A. 2012, ApJ, 760, 10
Herbig, G. H. 1975, ApJ, 196, 129
Hohle, M. M., Neuhäuser, R., & Schutz, B. F. 2010, Astron. Nachr., 331, 349
Huang, S.-S. 1972, ApJ, 171, 549
Hummel, W. 1994, A&A, 289, 458
Hummel, W., & Dachs, J. 1992, A&A, 262, L17
Hunt, L. K., Massi, M., & Zhekov, S. A. 1994, A&A, 290,
Hutchings, J. B., & Crampton, D. 1981, PASP, 93, 486
Johnston, S., Manchester, R. N., Lyne, A. G., et al. 1992, ApJ, 387, L37
Johnston, S., Manchester, R. N., Lyne, A. G., Nicastro, L., & Spyromilio, J. 1994, MNRAS, 268, 430
Liu, Q. Z., & Yan, J. Z. 2005, New Astron., 11, 130
Liu, Q. Z., Hang, H. R., Wu, G. J., Chang, J., & Zhu, Z. X. 2000, A&A, 359, 646
Lucarelli, F., Verrecchia, F., Striani, E., et al. 2010, ATel, 2761
Maier, G., & the VERITAS Collaboration 2015, ArXiv e-prints [arXiv:1508.05489]
Martin, R. G., Tout, C. A., & Pringle, J. E. 2009, MNRAS, 397, 1563
McSwain, M. V., Grundstrom, E. D., Gies, D. R., & Ray, P. S. 2010, ApJ, 724, 379
Meilland, A., Millour, F., Kanaan, S., et al. 2012, A&A, 538, A110
Morales-Rueda, L., Carter, D., Steele, I. A., Charles, P. A., & Worswick, S. 2004, Astron. Nachr., 325, 215
Moritani, Y., Nogami, D., Okazaki, A. T., et al. 2011, PASJ, 63, 25
Moritani, Y., Nogami, D., Okazaki, A. T., et al. 2013, PASJ, 65, 83
Moritani, Y., Okazaki, A. T., Carciofi, A. C., et al. 2015, ApJ, 804, L32
Munar-Adrover, P., Paredes, J. M., Ribó, M., et al. 2014, ApJ, 786, L11
Munari, U., & Zwitter, T. 1997, A&A, 318, 269
Negueruela, I., Ribó, M., Herrero, A., et al. 2011, ApJ, 732, L11
Okazaki, A. T., & Negueruela, I. 2001, A&A, 377, 161
Paredes, J. M., Marziani, P., Figueras, F., et al. 1990, Bol. Astron. Obs. Madrid, 12, 191
Paredes, J. M., Marziani, P., Marti, J., et al. 1994, A&A, 288
Paredes, J. M., Bednarek, W., Bordas, P., et al. 2013, Astropart. Phys., 43, 301
Porter, J. M. 1998, A&A, 333, L83
Porter, J. M., & Rivinius, T. 2003, PASP, 115, 1153
Puspitarini, L., Lallement, R., & Chen, H.-C. 2013, A&A, 555, A25
Quirrenbach, A., Bjorkman, K. S., Bjorkman, J. E., et al. 1997, ApJ, 479, 477
Rivinius, T., Carciofi, A. C., & Martayan, C. 2013, A&ARv, 21, 69
Robinson, R. D., & Smith, M. A. 2000, ApJ, 540, 474
Romero, G. E., Okazaki, A. T., Orellana, M., & Owocki, S. P. 2007, A&A, 474, 15
Saha, L., Chitnis, V. R., Shukla, A., Rao, A. R., & Acharya, B. S. 2016, ApJ, 823, 134
Shannon, R. M., Johnston, S., & Manchester, R. N. 2014, MNRAS, 437, 3255
Shrader, C. R., Hamaguchi, K., Sturner, S. J., et al. 2015, ApJ, 799, 84
Slettebak, A., Collins, G. W., II, & Truax, R. 1992, ApJS, 81, 335
Steele, I. A., Coe, M. J., Fabregat, J., et al. 1996, A&AS, 120, 213
Steele, I. A., Negueruela, I., Coe, M. J., & Roche, P. 1998, MNRAS, 297, L5
Steele, I. A., Smith, R. J., Rees, P. C., et al. 2004, Proc. SPIE, 5489, 679
Stoyanov, K. A., & Zamanov, R. K. 2009, Astron. Nachr., 330, 727
Straizys, V., & Kuriliene, G. 1981, Ap&SS, 80, 353
Swanenburg, B. N., Bennett, K., Bignami, G. F., et al. 1981, ApJ, 243, L69
Tycner, C., Gilbreath, G. C., Zavala, R. T., et al. 2006, AJ, 131, 2710
Wang, N., Johnston, S., & Manchester, R. N. 2004, MNRAS, 351, 599
Williams, S. J., Gies, D. R., Matson, R. A., et al. 2010, ApJ, 723, L93
Zamanov, R. K., & Martí, J. 2000, in The Be Phenomenon in Early-Type Stars, IAU Colloq. 175, ASP Conf. Proc., 214, 731
Zamanov, R. K., Martí, J., Paredes, J. M., et al. 1999, A&A, 351, 543
Zamanov, R., Stoyanov, K., Martí, J., et al. 2013, A&A, 559, A87
Zamanov, R., Stoyanov, K., Martí, J. 2016, Bulg. Astron. J., 24, 40